IEEE Access
Multidisciplinary | Rapid Review | Open Access Journal

Received February 26, 2019, accepted March 11, 2019, date of publication March 18, 2019, date of current version April 3, 2019.

Digital Object Identifier 10.1109/ACCESS.2019.2905416

Design of a Self-Complementary Frequency Selective Surface With Multi-Band Polarization Separation Characteristic

HUI WANG, MINGBAO YAN, SHAOBO QU, LIN ZHENG, AND JIAFU WANG
Department of Basic Science, Air Force Engineering University, Xi'an 710043, China

Corresponding authors: Mingbao Yan (mbyan2005@126.com), Shaobo Qu (qushaobo@mail.xjtu.edu.cn), and Lin Zheng (zhenglin0205@gmail.com)

This work was supported in part by the National Natural Science Foundation of China under Grant 61331005, Grant 61501502, Grant 61471388, and Grant 61771485, and in part by the National Key Research and Development Program of China under Grant 2017YFA07002015.

ABSTRACT According to the principle of Babinet, this paper designs a novel frequency selective surface (FSS) with high performance. Using the Babinet principle, an asymmetric Jerusalem cross patch structure and its complementary aperture structure are mixed on one side of the dielectric substrate, namely, self-complementary FSS (SCFSS). The theoretical analysis and experimental results show that SCFSS has excellent multi-bands polarization separation characteristics in different frequency ranges. In each passband, the insertion loss is less than 0.5 dB, and the out-of-band suppression level is relatively high. By individually adjusting the size of a certain structural parameter of SCFSS, the position of polarization separation frequency band can be adjusted in a specific frequency band range, thus meeting the requirements of the practical application. By rotating the surface, its filtering characteristics for polarized waves of a certain mode can be mechanically tuned from bandpass to bandstop. Furthermore, the SCFSS has an excellent incident angle stability in a wide range from 0° to 60°. Therefore, when designing polarization separation structure and polarization wave generator for the wireless communication system (such as the satellite communication system), the novel SCFSS structure proposed in this paper can provide an excellent reference.

INDEX TERMS Frequency selective surface, polarization separation, angle stability, multi-band.

I. INTRODUCTION

Frequency selective surface (FSS) is a planar array with two-dimensional periodic arrangement, which is constructed by metal patches or aperture units. FSS can reflect or transmit all the incident electromagnetic waves in certain frequency bands, showing extremely high frequency selective characteristics. Therefore, FSS presents the function of electromagnetic wave filter [1]–[4]. In order to reduce the radar cross section (RCS) of the target and achieve stealth effect [5]–[7], FSS-based composite absorbing materials [8]–[10] have been widely used in hybrid radomes. FSS has been widely used in the design of polarization mode converters and composite multi-frequency antennas in order to achieve high antenna utilization in parabolic antennas with sub-reflector [11], [12].

The associate editor coordinating the review of this manuscript and approving it for publication was Shagufta Henna.

In order to realize multi-frequency multiplexing in satellite communication, FSS is widely used in the design of multi-frequency multiplexers [13]. At present, the existence of various kinds of active interference and environmental clutter makes the electromagnetic environment extremely complex, which makes the transmission and detection capabilities of wireless multipath communication systems such as satellite communications decrease. Therefore, we need a polarization separation structure or a polarization wave generator to separate different polarization modes of electromagnetic waves or generate polarized electromagnetic waves in a single mode, so that the communication system can use polarization waves to load communication information in a single mode to resist interference of complex electromagnetic environment. However, the study on polarization separation characteristics of such FSS is rare [14]–[17]. Therefore, the generation of single-mode polarized electromagnetic waves in

wireless multipath communication systems requires a more in-depth study of the polarization separation characteristics of FSS [18], [19].

In recent years, people have proposed an interesting self-complementary frequency selective surface (SCFSS) (which remains the same when air and metal exchange) [20]. This structure only plays a role of polarization separation in one certain frequency band of millimeter wave band. Although the structure in [20] has good performance, because the unit size is equivalent to the resonant wavelength (this fact has an impact on the grating lobe), the structure provides an asymmetric passband and stopband (i.e. the resonant frequency of the passband is not consistent with the resonant frequency of the stopband) resulting in a relatively low frequency selectivity, which is not applicable if the goal is to design a bandpass/bandstop filter with high selectivity. In [21], a highly selective structure based on small self-complementary unit is theoretically proved, however, this structure has polarization separation characteristics only in one certain frequency band and has good passband and stopband symmetry when incident waves are perpendicularly incident. When incident at a large angle, the passband and stopband symmetry deteriorates, resulting in a rapid decrease in polarization selectivity. In addition, the same lumped circuit elements are widely used in this design. It is quite unrealistic to let these components not have parasitic effects, which is difficult to realize. Aiming at the problem of poor symmetry between passband and stopband when incident in large angle range. In [14], another structural form of frequency selection surface is proposed, which consists of structures complementary to the capacitive surface and the inductive surface to generate polarization separation response. The structure has stable angular response in a large angular range, and the pass band and the stop band are still symmetrical, so that the structure has high polarization selectivity. However, the polarization separation effect of this structure only exists in a certain frequency band, which limits its application range. In [15], the lumped LC device is loaded into the periodic array, and a polarization separation FSS structure is designed. The designed structure has stable angular response only in the 0°-40° scanning range of one certain frequency band, and provides symmetrical passband and stopband, so that the excellent polarization selection characteristics are well displayed in this structure. However, this structure is not suitable for large incident angle range.

Therefore, the design of polarization separation FSS still has many problems to be improved. Firstly, most of the existing polarization separation structures can only provide transmission passband/stopband for TE or TM polarization mode in a single frequency band, while it is impossible to simultaneously provide a single polarization mode transmission passband/stopband in multiple frequency bands. Therefore, these designs are difficult to meet the technical requirements of many wireless multi-path communication systems such as satellite communication and the like. Secondly, some polarization separation structures have poor symmetry between the passband and the stopband in the frequency band when the incident wave is incident vertically, making the polarization selectivity very low. Thirdly, although some polarization separation structures have better symmetry of passband and stopband when the incident wave is incident vertically, the symmetry effect of passband and stopband becomes worse under oblique incident angle.

In order to solve these problems, a multi-band polarization separation SCFSS structure is designed in this paper based on Babinet principle, which has stable angular response and good symmetry of passband/stopband in a large angle range from 0° to 60°. It is well known that metal strip gate structure can be used as polarization separator to separate TE polarization from TM polarization. In order to generate multiple polarization separation bands, the new zero point needs to be introduced. Therefore, on the basis of metal strip gate structure, SCFSS structure composed of asymmetric Jerusalem cross patch and its complementary aperture structure is introduced in order to facilitate structural size adjustment along x-direction and y-direction. Through structural size optimization adjustment, SCFSS provides polarization separation characteristics simultaneously in different frequency bands. In addition, SCFSS has a stable angular response in the range from 0° to 60°, and its passband and stopband remain symmetrical, so it has a relatively strong selection characteristic for electromagnetic waves and its out-of-band suppression level also maintains a relatively high standard. By individually adjusting the size of a certain structural parameter of SCFSS, the position of polarization separation frequency band can be adjusted in a specific frequency band range, thus meeting the requirements of practical application. By rotating the surface, its filtering characteristics can be mechanically tuned from bandpass to bandstop, so that the design update of the polarization separation structure and the polarization wave generator is more flexible and convenient.

It is worth noting that although the SCFSS structure designed in this paper and the structure proposed in [22] are both designed on the basis of asymmetric Jerusalem cross structure, the polarization separation characteristics of the structure are further studied. However, there are great differences between the two. First of all, the transmission mechanisms of the two structures are different. This paper is based on Babinet principle, while [22] is based on interlayer coupling principle. Secondly, the SCFSS structure proposed in this paper is a single-layer structure, simple, light and thin, which is more conducive to engineering applications. However, the structure in [22] is a multi-layer structure with relatively complex structure and limited application scope. Thirdly, the SCFSS structure proposed in this paper can complete polarization separation at the same resonant frequency point, but the structure in [22] cannot achieve this effect.

II. DESIGN OF SELF-COMPLEMENTARY FREQUENCY SELECTIVE SURFACE

It is well known that when the period of the metal strip gate structure is much shorter than the incident wavelength,

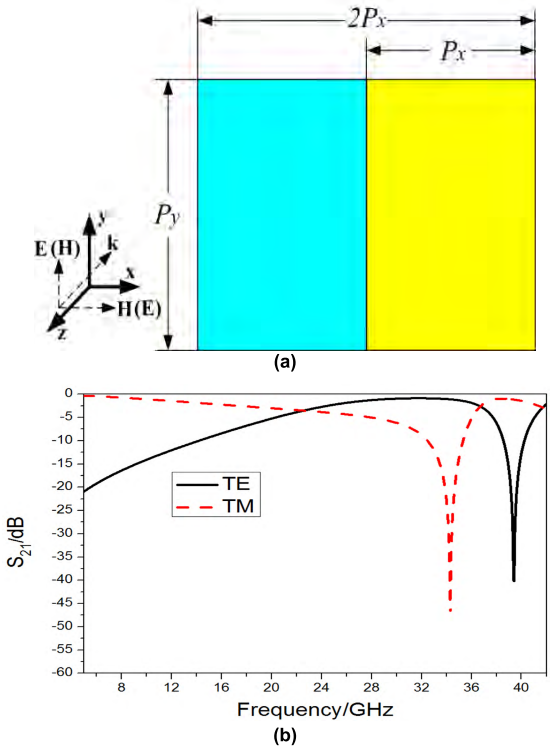

FIGURE 1. (a) Metal strip grid structure. (b) Under the condition of vertical incidence, the S_{21} curve obtained by simulating and calculating the structure shown in Fig. 1(a).

the metal strip gate structure acts as a polarization separator, separating TE polarization from TM polarization and providing a correct baseline for bandpass filtering and bandstop filtering [23]. Therefore, a metal strip gate structure is first designed as shown in Fig.1 (a), in which metal is represented by yellow parts and dielectric substrate is represented by blue parts. A material F4B-2 having a thickness h of 1.22mm, a relative dielectric constant ε_r of 2.65, and a loss tangent of 0.001 was used as a dielectric substrate. The other parameters of $P_x = 4$mm and $P_y = 5.7$mm. The CST simulation software is used for simulation calculation in this paper. The boundary condition of simulation is that periodic boundary is adopted in x-direction and y-direction. Fig. 1(b) shows a simulated S_{21} curve (in this paper, S_{21} refers to a transmission coefficient). As can be seen from Fig.1(b), the metal band gate structure separates TE polarization from TM polarization and introduces a zero point in the high frequency region of TE polarization and TM polarization, respectively.

In order to generate multiple polarization separated frequency bands, it is necessary to introduce a new zero point on the transmission curve of the metal strip gate structure. Therefore, an asymmetric Jerusalem cross structure is introduced on the left dielectric plate of the metal strip gate structure, and the structure is shown in Fig.2(a). The parameter values of the dielectric substrate using F4B-2 are unchanged. Other parameters are shown in Table 1. When TE wave and TM wave are incident vertically along the direction of wave vector k, the simulated result of S_{21} curve is shown in Fig.2 (b).

TABLE 1. Structural parameter values of the proposed SCFSS structure.

Structural parameter	P_x	P_y	L_1	L_2	S_1	S_2	M	N
Numerical (mm)	4	5.7	2.55	0.8	0.5	3.2	2.5	0.58

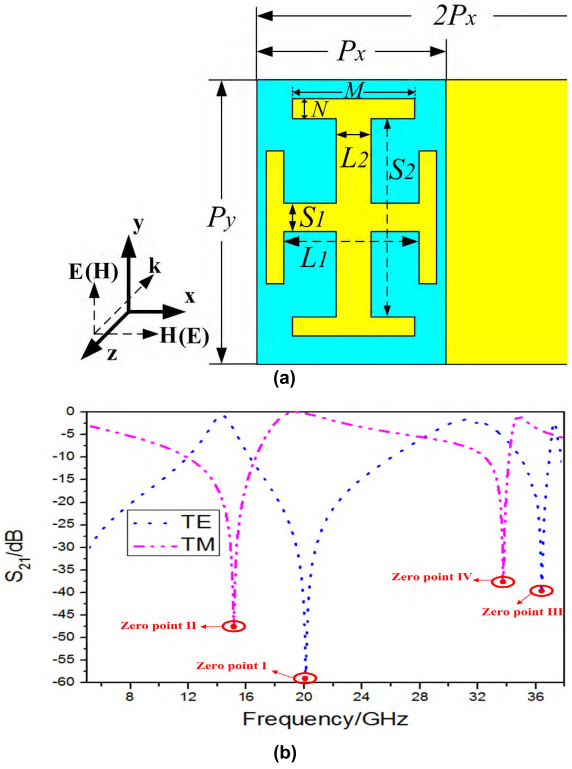

FIGURE 2. (a) The metal strip gate structure introduces the whole structure of asymmetric Jerusalem cross metal patch. (b) Under the condition of vertical incidence, the S_{21} curve obtained by simulating and calculating the structure shown in Fig. 2(a).

Since the asymmetric Jerusalem cross structure has different arm lengths along the x-direction and y- direction, it can introduce TE transmission zero point (i.e. the zero point I in Fig.2(b)) and TM transmission zero point (i.e. the zero point II in Fig.2(b)), respectively, in the transmission curve shown in Fig.1(b). Moreover, the different arm lengths of the Jerusalem cross structure also make the distance between the two introduced zeros be pulled apart, laying a foundation for the generation of multiple polarization separation bands.

As can be seen from Fig.2(b), both transmission zeros I and II are introduced by asymmetric Jerusalem cross structure, and the interval between the two zeros is large. Compared with the curve in Fig. 1(b), it can be seen that the zero point III and the zero point IV are obviously produced by the metal strip gate structure. However, the resonance points of the passband and the stopband are not consistent, and the passband and stopband symmetry is poor, so the polarization selection performance is poor.

As we know, the transmission characteristic of the aperture structure is bandpass effect, zero point will still be introduced at the high frequency of the passband. So the complementary aperture structure of asymmetric Jerusalem cross shown

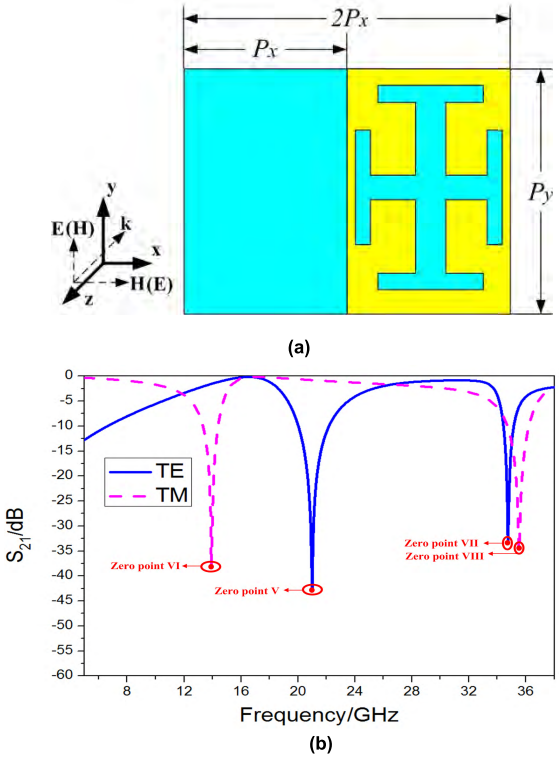

FIGURE 3. (a) The metal strip gate structure introduces an whole structure of asymmetric Jerusalem cross metal patch complementary aperture. (b) Under the condition of vertical incidence, the S_{21} curve obtained by simulating and calculating the structure shown in Fig.3(a).

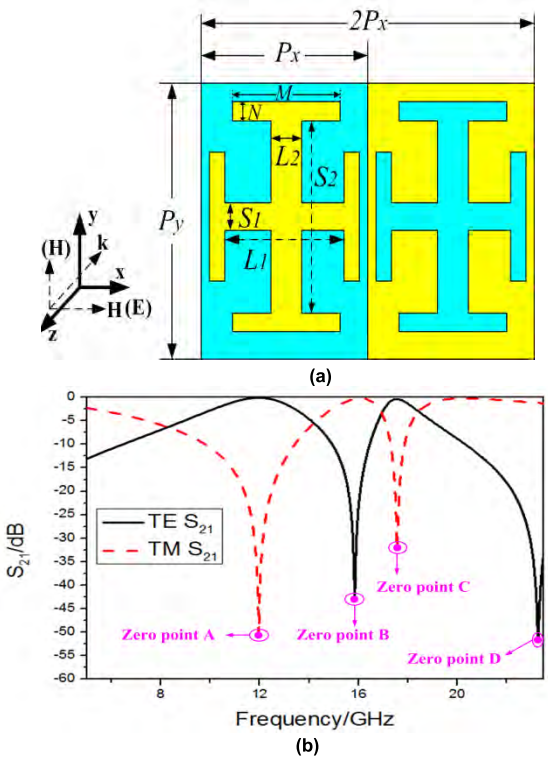

FIGURE 4. (a) The proposed SCFSS structure. (b). Under the condition of vertical incidence, the S_{21} curve obtained by simulating and calculating the structure shown in Fig.4(a).

in Fig.2(a) is introduced into the metal patch on the right side of the metal grid shown in Fig.1(a), then, the novel structure is shown in Fig.3 (a). The simulated result (S_{21} curve) is shown in Fig.3 (b).

Since the complementary aperture structure of the asymmetric Jerusalem cross metal patch has different aperture lengths along the x-direction and y-direction, it is also possible to introduce a TE polarization zero point and a TM polarization zero point, respectively, in the transmission curve shown in Fig. 1(b). As shown in Fig. 3(b), both the zero V and VI are introduced by the asymmetric Jerusalem cross patch and its complementary structure. Thus the distance between the two zero points is relatively large. Compared with the curve in Fig. 1(b), it can be seen that the zero point VII and the zero point VIII are obviously produced by the metal strip gate structure. However, the resonance points of the passband and the stopband are not consistent, so the polarization selection performance is poor.

It is known from Babinet principle that the metal patch and its complementary aperture structure should show strong response to TE mode and TM mode at the same resonance frequency [23], so we can apply Babinet principle to adjust the position of resonance points of both passband and stopband. Therefore, the asymmetric Jerusalem cross metal patch structure shown in Fig.2(a) and its complementary aperture structure shown in Fig. 3(a) are combined to form the SCFSS structure, as shown in Fig.4(a). The parameter values of the dielectric substrate using F4B-2 are unchanged. Other parameters are shown in Table 1. The simulated S_{21} curve is shown in Fig.4 (b).

Due to the complementary coupling between the metal patch structure and the aperture structure, according to Babinet principle, the TM zero A in Fig. 4(b) is obtained by adjusting and combining the TM zero II in Fig. 2(b) with the TM zero VI in Fig. 3(b). The TE zero B in Fig. 4(b) is obtained by adjusting and combining TE zero I in Fig. 2(b) and TE zero V in Fig. 3(b). The TM zero C in Fig. 4(b) is obtained by adjusting and combining the TM zero IV in Fig. 2(b) and TM zero VIII in Fig. 3(b). The TE zero point D in Fig. 4(b) is obtained by adjusting and combining the TE zero III in Fig. 2(b) and TE zero VII in Fig. 3(b). Because the size of the asymmetric Jerusalem cross patch and its complementary aperture structure can be adjusted in a larger range along the x-direction and y-direction relative to the self-complementary structure proposed in [20], [21], and [23], and the adjustment is more convenient. Therefore, we can get polarization separation transmission response in multiple frequency bands, the passband and stopband are symmetrical, thus greatly improving the polarization selection ability of the structure.

In Fig.5, Fig.6 and Fig.7, the induced current distributions of SCFSS units at three resonant frequencies $f_1 = 11.963$GHz, $f_2 = 15.845$GHz and $f_3 = 17.565$GHz are given respectively. These induced current distributions can help us understand the mechanism of resonance generation.

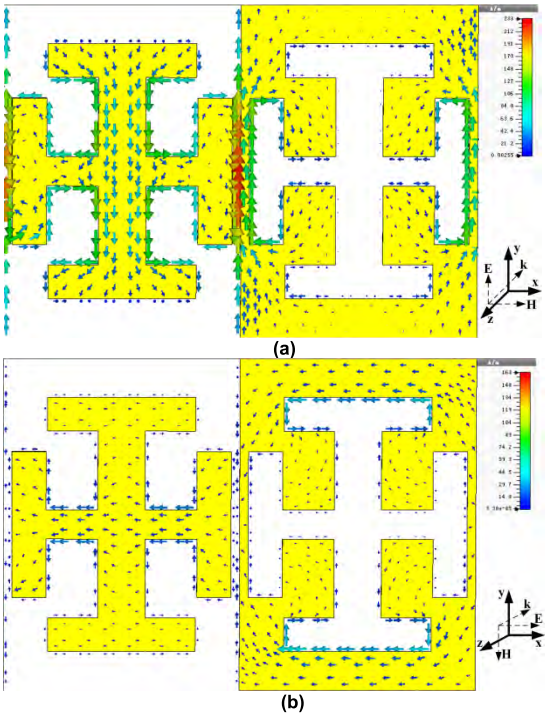

FIGURE 5. (a) At $f_1 = 11.963$GHz, the current distribution on the SCFSS structure surface under the vertical incidence of TE wave. (b) At $f_1 = 11.963$GHz, the current distribution on the SCFSS structure surface under the vertical incidence of TM wave.

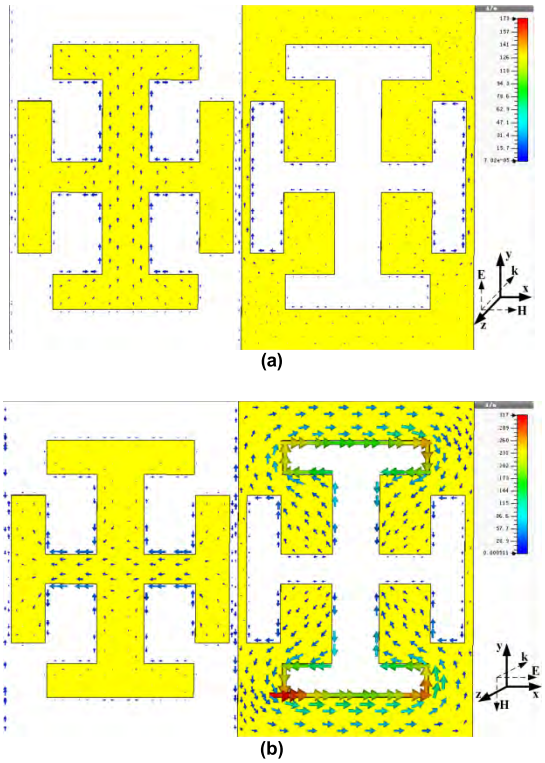

FIGURE 6. (a) At $f_2 = 15.845$GHz, the current distribution on the SCFSS structure surface under the vertical incidence of TE wave. (b) At $f_2 = 15.845$GHz, the current distribution on the SCFSS structure surface under the vertical incidence of TM wave.

The direction of current flow is indicated by arrows, dark color represents relatively strong current intensity, and light color represents relatively weak current intensity. Fig.5 shows the distribution of surface current of SCFSS unit under vertical incident wave at $f_1 = 11.963$GHz. As can be seen from Fig. 5(a), when TE wave is incident, along the y-direction, the asymmetric Jerusalem cross metal patch end line and its complementary aperture structure have a strong current distribution on the metal near the patch end line. The asymmetric Jerusalem cross metal patch terminal line and its complementary aperture structure have opposite current flows on the metal near the patch terminal line, resulting in strong electromagnetic coupling, thus generating first-order resonance. Therefore, the SCFSS transmission pole point at this time is caused by coupling resonance. From the above analysis, it can be seen that the polarization wave in TE mode can be transmitted due to the current excitation in y-direction of SCFSS structure. As can be seen from Fig.5(b), when TM wave is incident, the surface current distribution of the proposed SCFSS structure along the x-direction and y-direction are very weak and negligible.

Fig.6 shows the distribution of surface current of SCFSS unit under vertical incident wave at $f_2 = 15.845$GHz. It is seen from Fig.6(a), when TE wave is incident on, the surface current distribution of the proposed SCFSS structure along the x-direction and y-direction are very weak and negligible. As can be seen from Fig.6(b), when TM wave is incident on, along the x-direction, there is a strong current distribution on the edge of the terminal line aperture of the asymmetric Jerusalem cross complementary aperture structure. From the above analysis, it can be seen that the polarization wave in TM mode can be transmitted due to the current excitation in x-direction of SCFSS structure. Due to the same flow direction of surface current above the upper and lower end line edges of the aperture structure, considering the symmetry of the structure, we only need to discuss a section of induced currents. The surface current in the upper half of our aperture structure is taken as an example to illustrate the resonance principle: the surface current at the edge of the middle terminal line aperture is the strongest, and the surface current at the edge of the two end aperture structures is very weak or even zero. This current distribution is similar to the amplitude and node of a standing wave, and the electromagnetic wave is excited outward through the periodic oscillation of the induced current. Therefore, this resonance is called first order plasmon resonance [24]. Therefore, the SCFSS transmission pole point at this time is caused by the first order plasmon resonance.

Fig.7 shows the distribution of surface current of SCFSS unit under vertical incident wave at $f_3 = 17.565$GHz. As can be seen from Fig.7(a), when TE wave is incident on, along the y direction, there is a strong current distribution on the edge of the terminal line aperture of the asymmetric Jerusalem cross complementary aperture structure. From the above analysis, it can be seen that the polarization wave in TE mode can

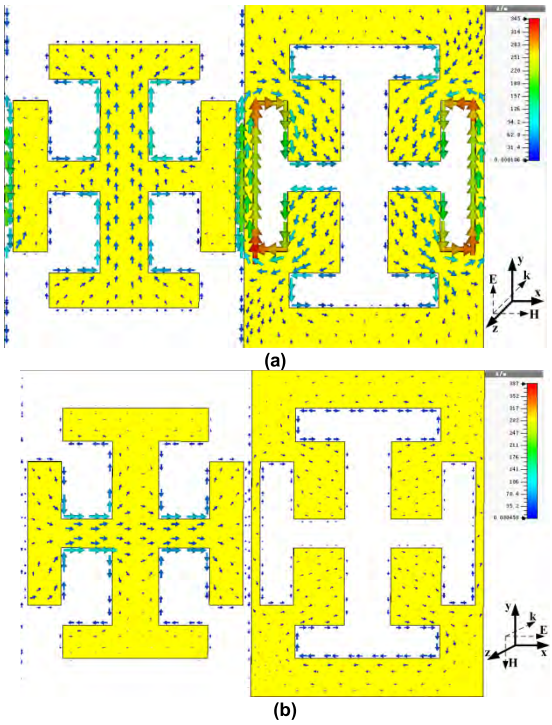

FIGURE 7. (a) At $f_3 = 17.565$GHz, the current distribution on the SCFSS structure surface under the vertical incidence of TE wave. (b) At $f_2 = 17.565$GHz, the current distribution on the SCFSS structure surface under the vertical incidence of TM wave.

be transmitted due to the current excitation in y-direction of SCFSS structure. Due to the same flow direction of surface current above the left and right end line edges of the aperture structure, considering the symmetry of the structure, we only need to discuss a section of induced currents. Similar to the analysis process of resonance mechanism in Fig.6(b), the transmission pole point of SCFSS structure in Fig.7(a) is also caused by first-order plasma resonance. As can be seen from Fig.7(b), when TM wave is incident on, the surface current distribution of the proposed SCFSS structure along the x-direction and y-direction are very weak and negligible.

From the above analysis, we can conclude that the asymmetry of the proposed SCFSS structure in the x-direction and y-direction play a crucial role in the selective transmission of TE and TM waves. Therefore, structural asymmetry can be widely used in designing polarization separation structures and polarization wave generators [22].

III. ANALYSIS OF FACTORS AFFECTING THE TRANSMISSION CHARACTERISTICS OF SCSFSS

As can be seen from the transmission curve shown in Fig. 4(b), for the proposed SCFSS, the insertion losses of the passbands in the three frequency bands are all less than 0.5dB. When the incident wave is incident vertically, the -3dB transmission operating bandwidth of TE polarized wave is 3.68GHz (9.87-13.55GHz) and 1.5GHz (16.94-18.44GHz), respectively, and the -3dB transmission operating bandwidth of TM polarized wave is 2.16GHz (14.78-16.94GHz). By observing each passband, it can be found that the amplitude variation of the falling edge of the transmission passband is not less than 5dB/GHz, and the falling edge of the passband is relatively steep. In three frequency bands, TE polarized wave and TM polarized wave respond simultaneously at the same resonance point in the frequency band, with one polarization mode reaching the pole while the other polarization mode reaching the zero point, i.e. the passband and stopband are symmetrical. It shows that TE wave and TM wave are perfectly separated in these three frequency bands, and the proposed SCFSS structure has a relatively strong selection characteristic for electromagnetic waves and its out-of-band suppression level also maintains a relatively high standard in these three frequency bands. Therefore, in specific multiple frequency bands, the SCFSS structure proposed in this paper realizes perfect separation of TE wave and TM wave.

A. INFLUENCE OF INCIDENT ANGLE CHANGE

In the analysis of this section, the transmission responses of TE polarized wave and TM polarized wave are simulated and calculated respectively by changing the incident angle, and the angular stability of SCFSS structure proposed in this paper under different polarized wave modes is deeply discussed. Keeping the structural parameters of SCFSS unchanged, the transmission curves obtained when TE and TM polarized waves are incident are shown in Fig.8(a) and Fig.8(b), respectively.

As can be seen from Fig.8, in the range of 0°-60° incidence angle, the transmission curve has the following characteristics with the change of incident wave polarization mode and incidence angle: (1) As shown in Fig. 8(a), when TE waves are incident and the angle increases, the position of the resonant frequency is relatively stable in the TE low-frequency passband, while the position of the resonant frequency in the TE high-frequency passband slightly drifts toward the low frequency direction. At the same time, the working bandwidth of both passbands is reduced and the out-of-band suppression capability is enhanced. The position of resonant frequency in TE stopband slightly drifts toward low frequency with the increase of incident angle, and the operating bandwidth slightly decreases. (2) As shown in Fig.8(b), when TM wave is incident and the angle increases, the position of the resonant frequency in the TM low-frequency stopband remains stable, while the position of the resonant frequency in the high-frequency stopband slightly drifts toward the low-frequency direction, and the operating bandwidth of the two stopbands slightly decreases. The position of resonant frequency in TM passband slightly drifts toward low frequency, the operating bandwidth slightly decreases, and the out-of-band suppression capability is enhanced.

From the above analysis, it can be found that with the increase of incident angle, both TE transmission curve and TM transmission curve change in the same direction, so that the resonance frequency position of TE polarization wave and TM polarization wave are consistent, i.e. the passband and stopband have good symmetry.

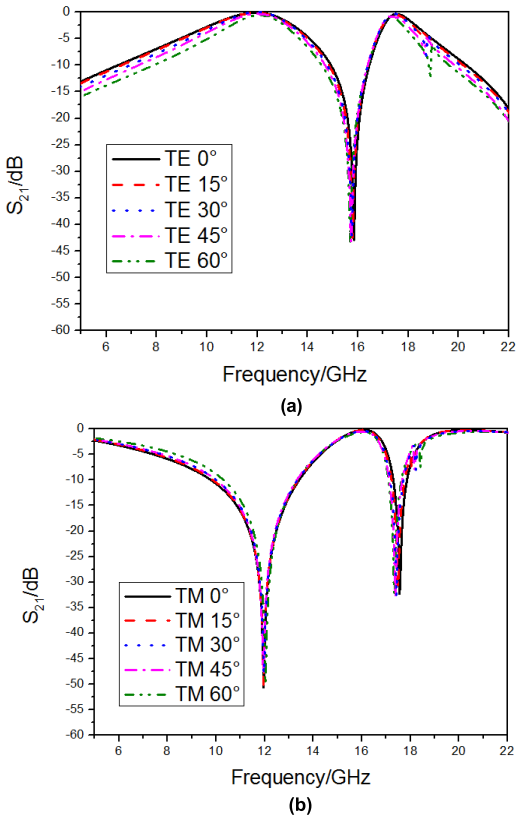

FIGURE 8. The transmission curves of TE polarized wave and TM polarized wave are obtained by simulation calculation under the premise of only changing the incident angle.

TABLE 2. Comparison of frequency shift at three resonance frequencies.

θ \ f	f_1=11.963GHz	f_2=15.845GHz	f_3=17.565GHz
Frequency shift（%）			
0°	0	0	0
15°	0	0	-0.06
30°	0	-0.05	-0.12
45°	-0.01	-0.12	-0.18
60°	-0.03	-0.16	-0.21

The frequency shift refers to the ratio of the working frequency of incident wave at oblique incidence to the working frequency of incident wave under normal incidence, and it is a physical quantity to measure the stability of transmission characteristics to incident angle. In Table 2, the amount of frequency shift of the three resonance frequencies when electromagnetic waves are incident is compared. In Table 2, "−" indicates movement to low frequencies. It can be seen from the table that the frequency shift when $f_1 = 11.963$GHz is negligible. When $f_2 = 15.845$GHz and $f_3 = 17.565$GHz, the shift of resonance frequency to low frequency increases slightly with the increase of incident angle θ, but the shift of frequency is very small. Therefore, the proposed SCFSS structure has a stable angular response.

Simulation results show that, in the range of 0° - 60°, the transmission response of the proposed SCFSS structure has good passband/stopband symmetry and excellent angular stability. Thus, we can see that the polarization separation characteristics of the SCFSS structure are very excellent.

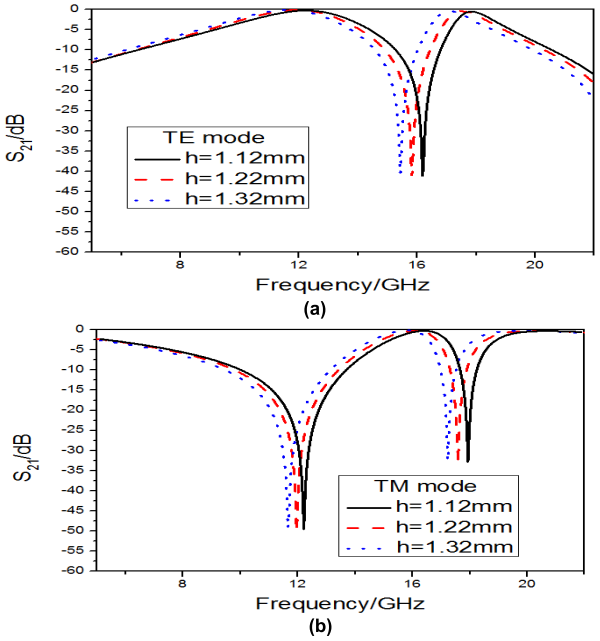

FIGURE 9. The transmission curves of TE polarized wave and TM polarized wave are obtained by simulation calculation under the premise of only changing the thickness h of the dielectric substrate when incident vertically.

B. INFIUENCE OF DIELECTRIC CHANGE

Firstly, the relative dielectric constant ε_r of the dielectric substrate is set to 2.65, and other parameters of the SCFSS structure proposed in this paper (as shown in Fig.4) remain unchanged. The thickness h of the dielectric substrate is set to 1.12 mm, 1.22 mm and 1.32 mm respectively, and then the parameters h of the SCFSS structure are scanned and calculated to obtain transmission characteristic results (as shown in Fig.9). Secondly, the thickness h of the dielectric substrate is set to 1.22mm and other parameters of the SCFSS structure proposed in this paper (as shown in Fig.4) remain unchanged. The relative dielectric constant ε_r of the dielectric substrate is set to 2.2, 2.65 and 3.1 respectively, and then the parameter ε_r of SCFSS structure is scanned and calculated to obtain the transmission characteristic result (as shown in Fig.10).

As can be seen from Fig.9, as the thickness h of the dielectric substrate increases, the TE transmission curve and TM transmission curve will simultaneously move toward the low frequency, and the resonance frequencies of the three frequency bands will also move toward the low frequency. The passband and stopband resonance frequencies in each frequency band are the same, the passband and stopband are still symmetrical, and the operating bandwidth of the passband/stopband is almost unchanged. Therefore, the frequency band can be shifted within a certain range by adjusting the thickness of the medium, and the polarization mode and bandpass/ bandstop mode of the desired frequency range can be selected.

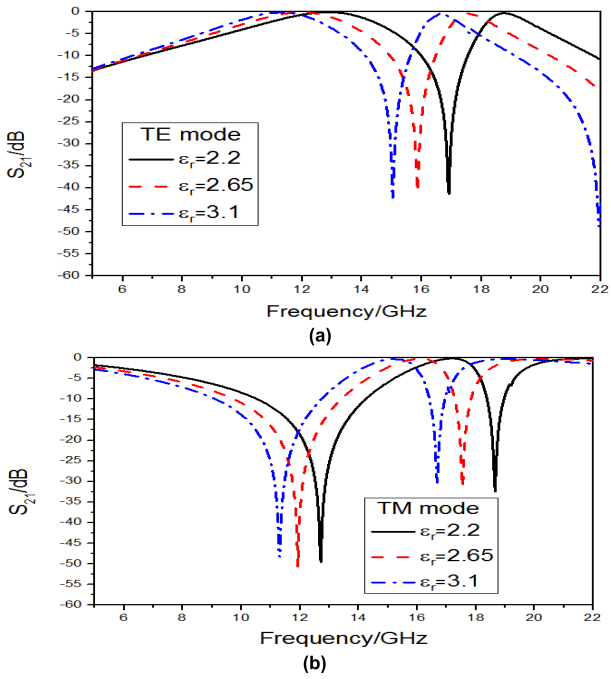

FIGURE 10. The transmission curves of TE polarized wave and TM polarized wave are obtained by simulation calculation under the premise of only changing the relative dielectric constants when incident vertically.

Looking at Fig.10, we can find that when TE wave and TM wave are perpendicularly incident on the SCFSS structure, when the relative dielectric constant of the dielectric substrate changes from small to large, the resonant frequency position in the dielectric gradually moves from high frequency to low frequency. We know that in Munk's FSS design theory, the relative dielectric constant ε_r of the dielectric has the following relationship with the resonant frequency f in the dielectric, $f = f_0/\sqrt{(1+\varepsilon_r)/2}$, where f_0 represents the resonant frequency in vacuum. from the formula, we find that the phenomenon produced by the transmission curve in Fig.10 is in accordance with Munk's theory.

In practical applications, it is often necessary to selectively transmit signals in the low-frequency region. Referring to the analysis results of the dielectric thickness h and the relative dielectric constant ε_r, we can try our best to select a dielectric with relatively thin thickness and relatively high relative dielectric constant as the substrate when designing FSS, so that the designed FSS can be pasted like wallpaper, making it more convenient to use FSS on irregular objects.

C. INFIUENCE OF SCFSS SIZE CHANGE

Through the above analysis, we know that the changes of long arm, short arm and end line of SCFSS structure play a crucial role in the transmission and selection of TE wave and TM wave. Therefore, the change of these structural dimensions will cause the position of the transmission curve to change accordingly, thus causing the corresponding transmission characteristics to change.

According to the model shown in Fig.4, only one parameter value is changed and the other parameters remain unchanged. We only change the short arm length L_1 or the long arm length S_2, or the end line length M or the end line width N of the asymmetric Jerusalem cross metal patch structure. At this time, the size of the complementary aperture structure of the asymmetric Jerusalem cross metal patch also changes accordingly. When the incident wave is incident vertically, the influence of the size change of different parameters on the transmission performance of SCFSS is shown in Fig.11. As can be seen from Figs.11(a)-(h), as these parameters gradually increase, the equivalent capacitance of SCFSS structure increases and the resonance frequency decreases. The TE transmission curve and TM transmission curve will move towards the low frequency at the same time, and the resonance frequencies of the three frequency bands will also move towards the low frequency. The operating bandwidths of both TE low-frequency passband and TM low-frequency stopband are slightly reduced, while the operating bandwidths of both TM passband and TE stopband are almost unchanged, while the operating bandwidths of both TE high frequency passband and TM high frequency stopband are slightly increased. The resonance frequencies of the passband and the stopband in each frequency band are the same, and the passband and the stopband are still symmetrical.

The SCFSS structure shown in Fig.4 is simulated and calculated. We only change the long arm width L_2 or the short arm width S_1 of the asymmetric Jerusalem cross metal patch structure. At this time, the size of the complementary aperture structure of the asymmetric Jerusalem cross metal patch also changes accordingly. When the incident wave is incident vertically, the influence of the size change of different parameters on the transmission performance of SCFSS is shown in Fig.12. As can be seen from Figs.12(a)-(d), as these parameters gradually increase, the equivalent capacitance of SCFSS structure decreases and the resonance frequency increases. The TE transmission curve and TM transmission curve will move towards the high frequency at the same time, and the resonance frequencies of the three frequency bands will also move towards the high frequency. The operating bandwidths of both TE low-frequency passband and TM low-frequency stopband are slightly increased, while the operating bandwidths of both TM passband and TE stopband are almost unchanged, while the operating bandwidths of both TE high-frequency passband and TM high-frequency stopband are slightly increased. The resonance frequencies of the passband and the stopband in each frequency band are the same, and the passband and and the stopband are still symmetrical.

Therefore, from the above analysis, we can move the frequency band within a certain frequency range by adjusting the parameter size of SCFSS structure, and we will select polarization mode and bandpass/bandstop mode in the required frequency range to meet the actual needs.

D. INFIUENCE OF SCFSS OVERALL ROTATION OF 90°

Rotate the overall structure of SCFSS by 90°. When TE wave and TM wave are incident vertically, its filtering characteristics can be mechanically tuned from bandpass to

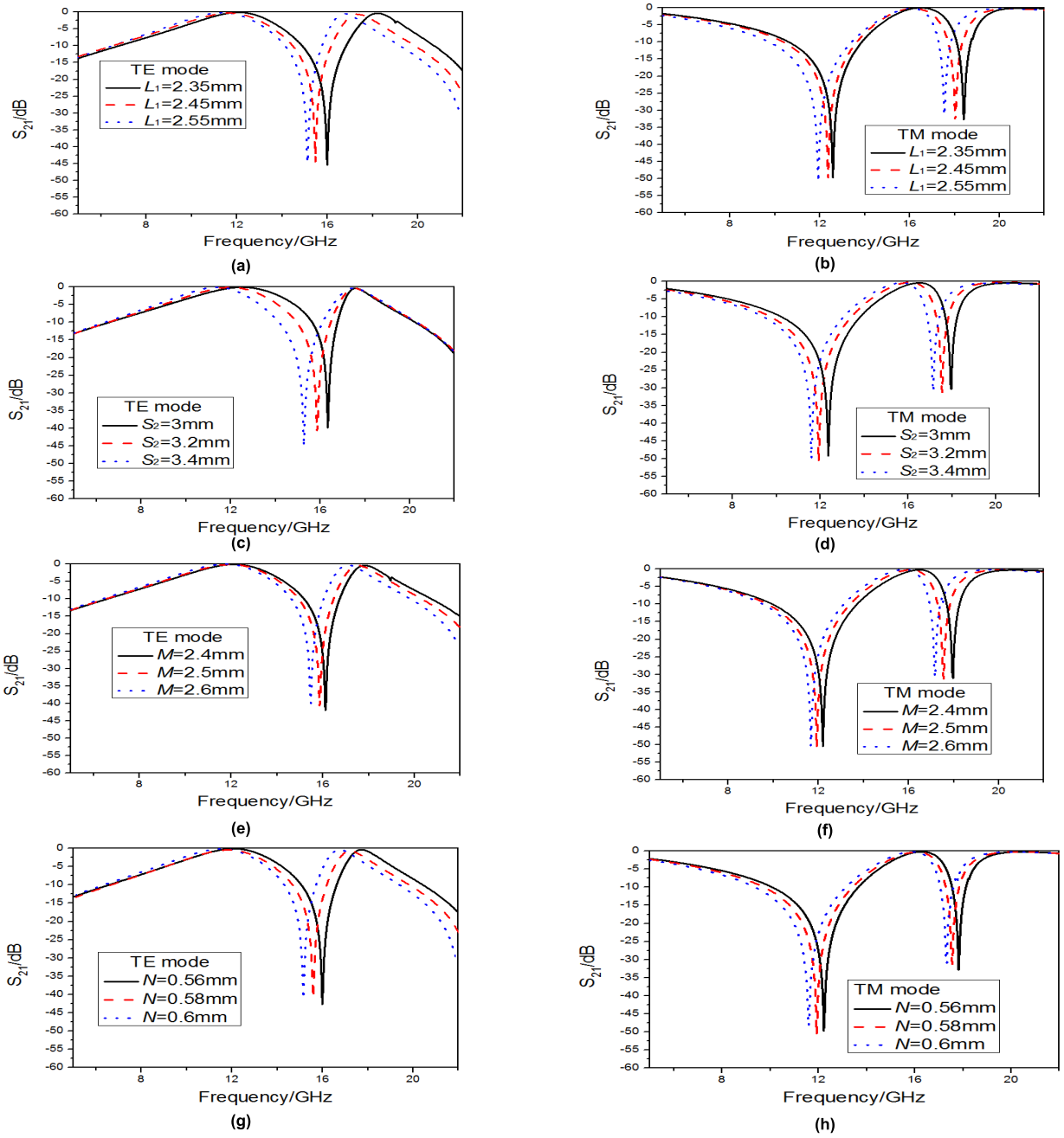

FIGURE 11. The transmission curves of TE polarized wave and TM polarized wave are obtained through simulation calculation on the premise that L_1, S_2, M and N are scanned respectively at vertical incidence.

bandstop. The transmission characteristic curve is shown in Fig.13. Comparing Fig.4 with Fig.13, we can find that the bandpass frequency band of TM polarized wave shown in Fig.13 replaces the bandpass frequency band of TE polarized waves shown in Fig.4, and the bandstop frequency band of TE polarized wave shown in Fig.13 replaces the bandstop frequency band of TM polarized waves shown in Fig.4, so that we can explain the occurrence of this phenomenon with reconfigurable characteristics. Through further analysis, it can be known that the SCFSS structure after the whole rotation of 90° still has good stability of large angle incidence (in the range of 0°-60° incidence angle) and excellent polarization separation characteristics (in the range of 0°-60° incidence angle). Therefore, if the above characteristics are applied to the design of polarization wave generator and polarization separation structure, the performance of FSS will be greatly improved.

IV. EXPERIMENTAL RESULTS

We carried out free space transmission measurements on SCFSS samples to verify the performance of SCFSS structures. The samples were prepared according to the

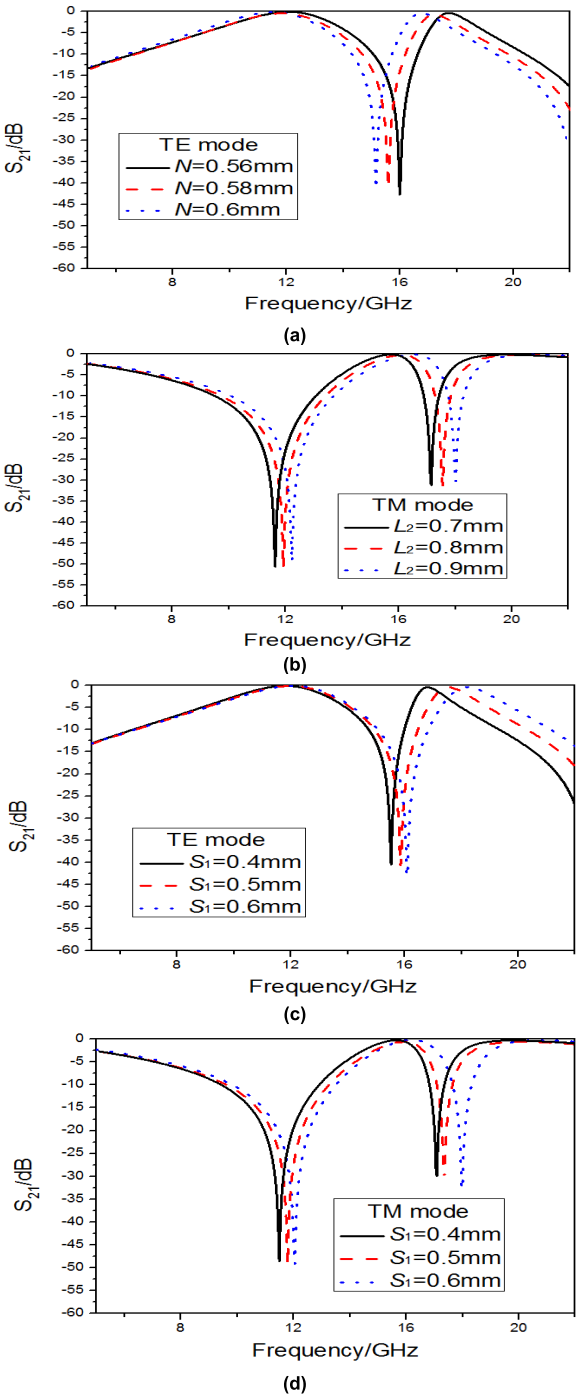

FIGURE 12. The transmission curves of TE polarized wave and TM polarized wave are obtained through simulation calculation on the premise that L_2 and S_1 are scanned respectively at vertical incidence.

SCFSS structure shown in Fig. 4 and the structural parameters shown in table 1, and the prepared samples are shown in Fig.14(b). The metal structure of SCFSS is etched on one side of the dielectric substrate by using printed circuit board technology. The prepared sample plate is $495.9 \times 496\ mm^2$ in size, including 87×62 SCFSS structural units. The free space measurement method is used for measurement. In order to ensure that TE polarized waves and TM polarized waves can

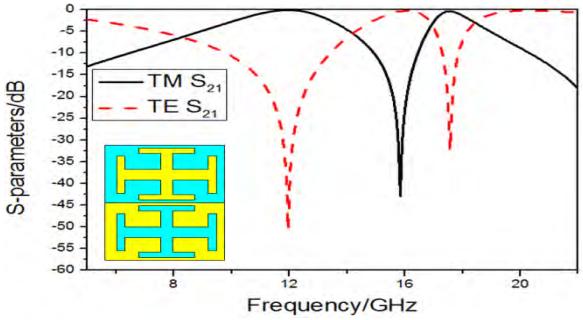

FIGURE 13. The transmission curves of TE polarized wave and TM polarized wave are obtained by simulation under the premise of only after SCFSS rotation 90° when incident vertically.

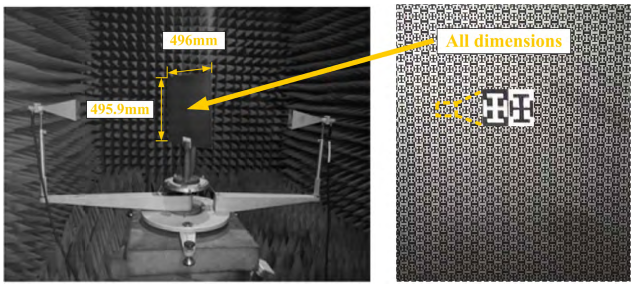

FIGURE 14. (a) The actual shooting pictures of the experimental measurement system. (b) The SCFSS samples manufactured.

both be incident on SCFSS samples in the form of quasi-plane waves and that the receiving antenna can effectively receive electromagnetic waves. The measurement was carried out in a microwave anechoic chamber and the SCFSS sample plate was placed between two double-ridge horn antennas already connected to a vector network analyzer (VNA). The actual shooting of the measurement location is shown in Fig.14(a). The distance from the position of the SCFSS sample plate to the two double ridge horn antennas is the same, both being 1.5m. The frequency range used in the measurement experiment is 1-25GHz. TE polarized wave and TM polarized wave are incident on SCFSS sample plate at incidence angles of 0°, 30° and 60° respectively. In order to minimize the interference and error caused by external environment and measurement system, the experiment will be guaranteed by normalization method.

On the premise of only changing the incident angle, the transmission curves of TE polarized wave and TM polarized wave are obtained through simulation and measurement as shown in Fig. 15. From Fig.15, we can see that in the range of 0°-60° incident angles, the measurement results of TE polarized wave transmission curve are basically consistent with the simulation results, and the measurement results of TM polarized wave transmission curve are also basically consistent with the simulation results. At the same time, we find that in the large incident angle range of 0°-60°, the passband and stopband of polarization separation transmission curve in the three frequency bands remain symmetrical, i.e. the TE wave resonance frequency position and TM wave resonance

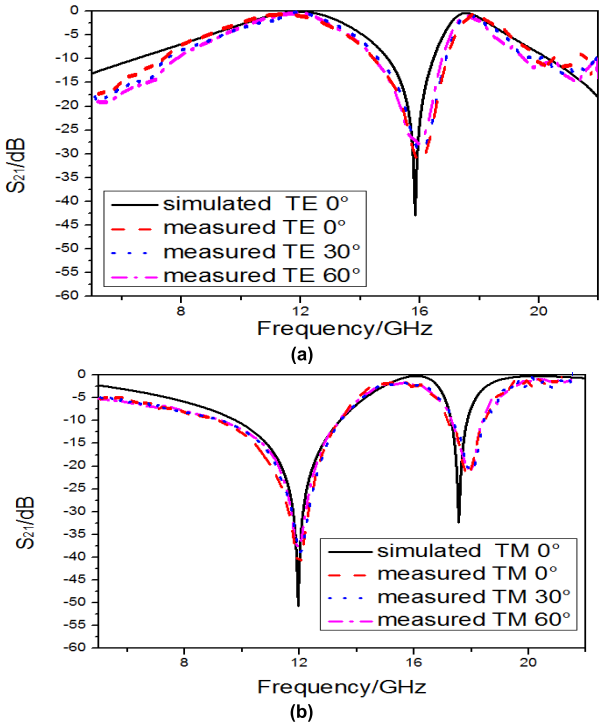

FIGURE 15. The transmission curves of TE polarized wave and TM polarized wave are obtained by simulation and measurement under the premise of only changing the incident angle. (a) TE polarization. (b) TM polarization.

TABLE 3. Comparing the proposed PSS with the performance of polarization separation structures proposed in the previous literature.

FSS structure	Whether multi-band polarization separation	Angular response stability(0°-60°)	Whether the passband and stopband are symmetric (0°-60°)
Structure in [14]	No	Stable	Yes
Structure in [15]	No	Unstable	No
Structure in [20]	No	Unstable	No
Structure in [21]	No	Unstable	No
Structure in [22]	Yes	Stable	No
The proposed PSS structure	Yes	Stable	Yes

frequency position keep consistent all the time, thus verifying the simulation result shown in Fig.8. The slight difference between the simulation results and the measurement results is mainly caused by the following three reasons: (1) There is an error between the etched metal structure on the sample and the simulation structure. (2) The dielectric substrate parameters used in the sample, such as thickness and relative dielectric constant, have errors with the simulation parameters. (3) There are errors in the operation and measurement systems during the experiment.

The experimental results show that the transmission curve of the proposed SCFSS structure has no grating lobe interference in the measurement frequency band range, and its passband and stopband have good symmetry, and the transmission has high polarization selectivity, good large-angle incident stability and stable polarization separation characteristics in a large-angle range. It provides a good reference for the design of structures with linear polarization selection characteristics. Comparing the performance of the proposed PSS structure with that of the polarization separation structure proposed in previous documents, as shown in Table 3, it can be seen that the PSS structure proposed in this paper has strong novelty and improvement.

V. CONCLUSION

Based on the strip metal grid structure and Babinet principle, this paper designs a single-layer multi-band polarization separation structure consisting of asymmetric Jerusalem cross metal patch and its complementary aperture structure, called self-complementary frequency selective surface (SCFSS) structure. When the TE polarized wave and TM polarized wave are incident vertically, the TE passband and TM stopband are generated in the 9.87GHz-13.55GHz band and the 16.94GHz-18.44GHz band, and the TM passband and TE stopband are generated in the 14.78GHz-16.94GHz band. And in three frequency bands, TE wave and TM wave respond simultaneously at the same resonance point, that is, one mode reaches the pole while the other mode reaches the zero point, and the passband and stopband are symmetrical. Through simulation calculation and experimental verification, it can be concluded that good polarization separation characteristics, high out-of-band suppression level, stable angular response at large angle(0°-60°) incidence, and good passband and stopband symmetry at large angle range(0°-60°) are all excellent characteristics of the proposed SCFSS structure. In a certain frequency range, the frequency band can be shifted by adjusting the parameter size of SCFSS structure, and the polarization mode and bandpass/bandstop mode in the required frequency range can be selected according to the actual application requirements. Furthermore, without changing the structural parameters of SCFSS, we rotate the whole SCFSS by 90° . We can mechanically tune the filtering characteristics of TE mode and TM mode, i.e. let their bandpass and bandstop states exchange with each other. From the above, the novel structure proposed in this paper can provide a good reference for the design of polarization separation structure and polarization wave generator in wireless communication systems (such as satellite communication systems).

REFERENCES

[1] B. A. Munk, *Frequency Selective Surfaces: Theory and Design*. New York, NY, USA: Wiley, 2000.
[2] T. K. Wu, *Frequency Selective Surface and Grid Array*. New York, NY, USA: Wiley, 1995.
[3] A. Ferraro, D. C. Zografopoulos, R. Caputo, and R. Beccherelli, "Periodical elements as low-cost building blocks for tunable terahertz filters," *IEEE Photon. Technol. Lett.*, vol. 28, no. 21, pp. 2459–2462, Nov. 1, 2016.
[4] V. Sanphuang, N. Ghalichechian, N. K. Nahar, and J. L. Volakis, "Reconfigurable THz filters using phase-change material and integrated heater," *IEEE Trans. THz Sci. Technol.*, vol. 6, no. 4, pp. 583–591, Jul. 2016.

[5] Q. Chen and Y. Fu, "A planar stealthy antenna radome using absorptive frequency selective surface," *Microw. Opt. Technol. Lett.*, vol. 56, no. 8, pp. 1788–1792, Aug. 2014.

[6] M. Yan *et al.*, "A tri-band, highly selective, bandpass FSS using cascaded multilayer loop arrays," *IEEE Trans. Antennas Propag.*, vol. 64, no. 5, pp. 2046–2049, May 2016.

[7] M. Yan *et al.*, "A miniaturized dual-band FSS with stable resonance frequencies of 2.4 GHz/5 GHz for WLAN applications," *IEEE Antennas Wireless Propag. Lett.*, vol. 13, pp. 895–898, 2014.

[8] Q. Chen, L. Liu, L. Chen, J. Bai, and Y. Fu, "Absorptive frequency selective surface using parallel LC resonance," *Electron. Lett.*, vol. 52, no. 6, pp. 418–419, Mar. 2016.

[9] Q. Chen, J. J. Bai, L. Chen, and Y. Q. Fu, "A miniaturized absorptive frequency selective surface," *IEEE Antennas Wireless Propag. Lett.*, vol. 14, pp. 80–83, 2015.

[10] W. Yuan, Q. Chen, Y. Xu, H. Xu, S. Bie, and J. Jiang, "Broadband microwave absorption properties of ultrathin composites containing edge-split square-loop FSS embedded in magnetic sheets," *IEEE Antennas Wireless Propag. Lett.*, vol. 16, pp. 278–281, 2017.

[11] B. Lin, J.-L. Wu, X.-Y. Da, W. Li, and J.-J. Ma, "A linear-to-circular polarization converter based on a second-order band-pass frequency selective surface," *Appl. Phys. A, Solids Surf.*, vol. 123, p. 43, Jan. 2017.

[12] D. Wang, W. Che, Y. Chang, K.-S. Chin, and Y. L. Chow, "Combined-element frequency selective surfaces with multiple transmission poles and zeros," *IET Microw., Antennas Propag.*, vol. 8, no. 3, pp. 186–193, Feb. 2014.

[13] Y. Rahmat-Samii and A. C. Densmore, "Technology trends and challenges of antennas for satellite communication systems," *IEEE Trans. Antennas Propag.*, vol. 63, no. 4, pp. 1191–1204, Apr. 2015.

[14] J. Jiao, J.-S. Gao, N.-X. Xu, and X. Chen, "Design and study of the polarization selective surface based on the complementary screens," *Acta Phys. Sinica*, vol. 62, no. 19, pp. 446–453, 2013.

[15] X.-Z. Wang, J.-S. Gao, and N.-X. Xu, "Characteristics of polarization separation of frequency selective surface by lumped inductors and capacitors," *Acta Phys. Sinica*, vol. 62, no. 14, pp. 1005–1012, 2013.

[16] H. Li, Y. Li, Y. Wang, and Q. Cao, "A multifunctional active frequency selective surface with parallel feed network," in *Proc. Int. Workshop Electromagn., Appl. Student Innov. Competition*, London, U.K., May/Jun. 2017, pp. 93–94.

[17] H. Li, Q. Cao, and Y. Wang, "A novel 2-B multifunctional active frequency selective surface for LTE-2.1 GHz," *IEEE Trans. Antennas Propag.*, vol. 65, no. 6, pp. 3084–3092, Jun. 2017.

[18] M.-A. Joyal and J.-J. Laurin, "A cascaded circular-polarization-selective surface at K band," in *Proc. IEEE Int. Symp. Antennas Propag.*, Jul. 2011, pp. 2657–2660.

[19] R. Orr *et al.*, "Circular polarization frequency selective surface operating in ku and Ka band," *IEEE Trans. Antennas Propag.*, vol. 63, no. 11, pp. 5194–5197, Nov. 2015.

[20] M. Beruete, M. N. CÍa, I. Campillo, P. Goy, and M. Sorolla, "Quasioptical polarizer based on self-complementary sub-wavelength hole arrays," *IEEE Microw. Wireless Compon. Lett.*, vol. 17, no. 12, pp. 834–836, Dec. 2007.

[21] J. D. Ortiz, J. D. Baena, R. Marqués, and F. Medina, "A band-pass/stop filter made of SRRs and C-SRRs," in *Proc. IEEE Int. Symp. Antennas Propag. (APSURSI)*, Spokane, WA, USA, Jul. 2011, pp. 2669–2672.

[22] H. Wang, L. Zheng, M. Yan, J. Wang, S. Qu, and R. Luo, "Design and analysis of miniaturized low profile and second-order multi-band polarization selective surface for multipath communication application," *IEEE Access*, vol. 7, pp. 13455–13467, 2019.

[23] J. D. Ortiz, J. D. Baena, V. Losada, F. Medina, R. Marqués, and J. L. A. Quijano, "Self-complementary metasurface for designing narrow band pass/stop filters," *IEEE Microw. Wireless Compon. Lett.*, vol. 23, no. 6, pp. 291–293, Jun. 2013.

[24] M. Feng, J. Wang, H. Ma, W. Mo, H. Ye, and S. Qu, "Broadband polarization rotator based on multi-order plasmon resonances and high impedance surfaces," *J. Appl. Phys.*, vol. 114, Aug. 2013, Art. no. 074508.

HUI WANG received the B.S. and M.S. degrees in communication engineering from Xidian University, Xi'an, Shaanxi, China, in 2008 and 2013, respectively. He is currently pursuing the Ph.D. degree in electronic science and technology with Air Force Engineering University, Xi'an. He conducted research under the guidance of Prof. S. Qu. His research interests include frequency selective surface and radome.

MINGBAO YAN received the B.S. and M.S. degrees in physics from Qufu Normal University, Qufu, China, in 2005 and 2008, respectively, and the Ph.D. degree in physical electronics from Air Force Engineering University, Xi'an, Shaanxi, China, in 2016. Since 2008, he has been with Air Force Engineering University, where he is currently an Associate Professor in physical electronics. His current research interests include frequency selective surface and the design of stealth radome metamaterial.

SHAOBO QU received the B.S. degree in physics from Fuyang Normal College, Fuyang, Anhui, China, in 1984, the M.S. degree in physics from Sichuan Normal University, Chengdu, China, in 1991, and the Ph.D. degree in materials science and engineering from Northwest Polytechnical University, Xi'an, China, in 2001. Since 2001, he has been with the Department of Applied Mathematics and Physics, Air Force Engineering University, Xi'an, where he is currently a Professor in physical electronics. His research interests include materials physics, metamaterials, and electronic materials and devices.

LIN ZHENG was born in 1986. He received the Ph.D. degree in electronics science and technology from Air Force Engineering University, Xi'an, Shaanxi, China, in 2015, where he is currently with the Department of Basic Sciences. His research direction is frequency selective surface, metamaterial, and radome.

JIAFU WANG received the B.S. degree in radar engineering, the M.S. degree in optics engineering, and the Ph.D. degree in physical electronics from Air Force Engineering University, Xi'an, in 2004, 2007 and 2010, respectively, where he is currently an Associate Professor in physical electronics. His current research interests include plasma stealth, design of metamaterials, and application of the metamaterials in microwave devices.